Progress of Theoretical Physics, Vol. 106, No. 6, December 2001

Linear Σ Model in the Gaussian Functional Approximation

Issei NAKAMURA and V. DMITRAŠINOVIĆ*)

Research Center for Nuclear Physics, Osaka University, Ibaraki 567-0047, Japan

(Received June 15, 2001)

We apply a self-consistent relativistic mean-field variational "Gaussian functional" (or Hartree) approximation to the linear σ model with spontaneously and explicitly broken chiral $O(4)$ symmetry. We set up the self-consistency, or "gap" and the Bethe-Salpeter equations. We check and confirm the chiral Ward-Takahashi identities, among them the Nambu-Goldstone theorem and the (partial) axial current conservation [CAC], both in and away from the chiral limit. With explicit chiral symmetry breaking, we confirm the Dashen relation for the pion mass and partial CAC. We solve numerically the gap and Bethe-Salpeter equations, discuss the solutions' properties and the particle content of the theory.

§1. Introduction

The Gell-Mann–Levy [GML] linear sigma model has long been a subject of nonperturbative studies, both for its particle physics and statistical mechanics applications.[1),2)] In this paper we apply a new chirally invariant version of the Lorentz invariant self-consistent mean-field variational approximation that goes by many names, *inter alia* the Gaussian functional approximation[3),4)] to the linear sigma model. The improvement that we present in this paper is the correct implementation of the chiral symmetry in this approximation. We prove the chiral Ward-Takahashi identities, among them the Nambu-Goldstone theorem, the Dashen relation, and the axial current (partial) conservation (PCAC) in this approximation. Then we present a numerically obtained solution of the gap and Bethe-Salpeter equations and discuss the particle content of the theory in this approximation.

Our motivation for this study is the desire to publicize progress made in understanding the Gaussian approximation, which is often used in finite temperature/density applications,[5),6)] albeit often in incomplete form, and the hope that this work will ultimately lead to the clarification of the scalar meson spectroscopy, and in particular of the so-called σ meson. For this reason, the present study of the GML model must be considered as a methodological work providing preparatory for a full-fledged, $N_f = 3$ calculation.

This paper consists of six sections. In §2 we introduce the linear Σ model. In §3 we outline the Gaussian approximation, and in §4 we demonstrate its chiral invariance. In §5 we present results of the numerical solution of the gap and the Bethe-Salpeter equations and analyze the solutions. Finally, we summarize and draw conclusions in §6.

*) Address after 1st July 2001: Vinča Institute of Nuclear Sciences, P. O. Box 522, 11001 Belgrade, Yugoslavia.

§2. The linear Σ model

We confine ourselves to the $O(N=4)$ symmetric linear σ model for the sake of simplicity. The Lagrangian density of this theory is

$$\mathcal{L} = \frac{1}{2}\left(\partial_\mu \boldsymbol{\phi}\right)^2 - V(\boldsymbol{\phi}^2)\ , \tag{2·1}$$

where

$$\boldsymbol{\phi} = (\phi_0, \phi_1, \phi_2, \phi_3) = (\sigma, \boldsymbol{\pi})$$

is a column vector and

$$V(\boldsymbol{\phi}^2) = -\frac{1}{2}\mu_0^2\boldsymbol{\phi}^2 + \frac{\lambda_0}{4}\left(\boldsymbol{\phi}^2\right)^2 .$$

We assume here that λ_0 and μ_0^2 are not only positive, but such that spontaneous symmetry breakdown (SSB) occurs in the mean-field approximation [MFA], to be introduced below. As the chiral symmetry breaking (χSB) term in the Lagrangian, we choose

$$\mathcal{L}_{\chi\mathrm{SB}} = -\mathcal{H}_{\chi\mathrm{SB}} = \varepsilon\sigma, \tag{2·2}$$

as suggested by the underlying NJL quark model. The interaction potential in the new field variable $s \equiv \sigma - \langle\sigma\rangle_{0\mathrm{B}}$ reads

$$\begin{aligned} V = &\frac{1}{2}\left(m_{\sigma\mathrm{B}}^2 s^2 + m_{\pi\mathrm{B}}^2\boldsymbol{\pi}^2\right) + \left(\frac{m_{\sigma\mathrm{B}}^2 - m_{\pi\mathrm{B}}^2}{2f_{\pi\mathrm{B}}}\right) s\left(s^2+\boldsymbol{\pi}^2\right) \\ &+ \left(\frac{m_{\sigma\mathrm{B}}^2 - m_{\pi\mathrm{B}}^2}{8f_{\pi\mathrm{B}}^2}\right)\left(s^2+\boldsymbol{\pi}^2\right)^2 . \end{aligned} \tag{2·3}$$

The scalar meson (σ) mass, the vacuum expectation value (v.e.v.) and the pion ($\boldsymbol{\pi}$) mass are

$$\langle\sigma\rangle_{0\mathrm{B}} = v_{\mathrm{B}} = f_{\pi\mathrm{B}} = -\frac{\varepsilon}{\mu_0^2} + \lambda_0\frac{v_{\mathrm{B}}^3}{\mu_0^2}\ , \tag{2·4a}$$

$$m_{\sigma\mathrm{B}}^2 = -\mu_0^2 + 3\lambda_0 f_{\pi\mathrm{B}}^2\ , \tag{2·4b}$$

$$m_{\pi\mathrm{B}}^2 = -\mu_0^2 + \lambda_0 f_{\pi\mathrm{B}}^2 = \frac{\varepsilon}{v_{\mathrm{B}}}\ . \tag{2·4c}$$

Note that once the pion mass $m_{\pi\mathrm{B}}$ and decay constant $f_{\pi\mathrm{B}}$ have been fixed, there is only one free parameter left in this (tree) approximation, the scalar meson σ mass $m_{\sigma\mathrm{B}}$. The quartic coupling constant λ_0 can be expressed as

$$\lambda_0 = \left(\frac{m_{\sigma\mathrm{B}}^2 - m_{\pi\mathrm{B}}^2}{2f_{\pi\mathrm{B}}^2}\right)\ . \tag{2·5}$$

This relation is a powerful result, as it implies a cubic dependence of the σ decay width on its mass:

$$\Gamma_{\sigma\pi\pi} = 3\frac{\left(m_{\sigma\mathrm{B}}^2 - m_{\pi\mathrm{B}}^2\right)^2}{32\pi f_{\pi\mathrm{B}}^2 m_{\sigma\mathrm{B}}}\sqrt{1-\left(\frac{2m_{\pi\mathrm{B}}}{m_{\sigma\mathrm{B}}}\right)^2}\ . \tag{2·6}$$

Therefore, as soon as the σ mass exceeds the two-pion threshold, the decay width increases so quickly that instead of a sharp "peak" in the cross section there is a broad "bump", unrecognizable as a resonance. This fact is a consequence of the strong coupling implied by Eq. (2·5), which in turn is a consequence of the linear realization of the chiral symmetry in the Born approximation. Here, natural (and long-standing) questions arise: Does this effect survive after taking into account the loop corrections? What kind of a particle, if any, corresponds to the σ field, and how does one identify it? Many studies have been devoted to answering these questions, but most suffer from either being perturbative, which is unacceptable in the strong coupling case, or from not being chirally symmetric. We satisfy both of these requirements by employing the non-perturbative, chirally symmetric method described in the next section.

§3. The Gaussian variational method

Over the past 20 years we have seen the relativistic Rayleigh-Ritz variational approximation based on the Gaussian ground state (vacuum) functional elevated from a little-known specialist technical tool [3] to a textbook method. [4] This method sometimes also goes by the names 'self-consistent mean field approximation' (MFA) and 'Hartree + RPA'.*) In the following we use these terms interchangeably.

3.1. *The basics of the Gaussian functional approximation*

We use the Gaussian ground state functional Ansatz

$$\Psi_0[\vec{\phi}] = \mathcal{N} \exp\left(-\frac{1}{4\hbar}\int d\boldsymbol{x}\int d\boldsymbol{y}\,[\phi_i(\boldsymbol{x})-\langle\phi_i(\boldsymbol{x})\rangle]\,G^{-1}_{ij}(\boldsymbol{x},\boldsymbol{y})\,[\phi_j(\boldsymbol{y})-\langle\phi_j(\boldsymbol{y})\rangle]\right)\,, \tag{3·1}$$

where $\mathcal{N}$ is the normalization constant, $\langle\phi_i(\boldsymbol{x})\rangle$ is the vacuum expectation value (v.e.v.) of the i-th spinless field (which henceforth we will assume to be translationally invariant, $\langle\phi_i(\boldsymbol{x})\rangle = \langle\phi_i(0)\rangle \equiv \langle\phi_i\rangle$), and

$$G_{ij}(\boldsymbol{x},\boldsymbol{y}) = \frac{1}{2}\delta_{ij}\int\frac{d\boldsymbol{k}}{(2\pi)^3}\frac{1}{\sqrt{\boldsymbol{k}^2+m_i^2}}e^{i\boldsymbol{k}\cdot(\boldsymbol{x}-\boldsymbol{y})}.$$

Furthermore, note that we have explicitly kept $\hbar$ (while setting the velocity of light $c=1$) to keep track of quantum corrections and count the number of "loops" in our calculation. Then the "vacuum" (ground state) energy density becomes

$$\begin{aligned}\mathcal{E}(m_i,\langle\phi_i\rangle) = &-\varepsilon\langle\phi_0\rangle - \frac{1}{2}\mu_0^2\langle\boldsymbol{\phi}\rangle^2 + \frac{\lambda_0}{4}\left[\langle\boldsymbol{\phi}\rangle^2\right]^2\\ &+\hbar\sum_i\left[I_1(m_i)-\frac{1}{2}\mu_0^2 I_0(m_i)-\frac{1}{2}m_i^2 I_0(m_i)\right]\end{aligned}$$

*) Due to the Bose statistics of our fields and the covariance of our approach, RPA might be equivalent to the Tamm-Dancoff approximation (TDA) in this case.

$$+\frac{\lambda_0}{4}\Bigg\{6\hbar\sum_i\langle\phi_i\rangle^2 I_0(m_i)+2\hbar\sum_{i\neq j}\langle\phi_i\rangle^2 I_0(m_j)$$
$$+3\hbar^2\sum_i I_0^2(m_i)+2\hbar^2\sum_{i<j}I_0(m_i)I_0(m_j)\Bigg\}\ , \qquad (3\cdot2)$$

where

$$I_0(m_i)=\frac{1}{2}\int\frac{d\boldsymbol{k}}{(2\pi)^3}\frac{1}{\sqrt{\boldsymbol{k}^2+m_i^2}}=i\int\frac{d^4k}{(2\pi)^4}\frac{1}{k^2-m_i^2+i\epsilon}=G_{ii}(\boldsymbol{x},\boldsymbol{x})\ , \qquad (3\cdot3)$$

$$I_1(m_i)=\frac{1}{2}\int\frac{d\boldsymbol{k}}{(2\pi)^3}\sqrt{\boldsymbol{k}^2+m_i^2}=-\frac{i}{2}\int\frac{d^4k}{(2\pi)^4}\log\left(k^2-m_i^2+i\epsilon\right)+\text{const.} \qquad (3\cdot4)$$

We identify $\hbar I_1(m_i)$ with the familiar "zero-point" energy density of a free scalar field of mass m_i.

The divergent integrals $I_{0,1}(m_i)$ are understood to be regularized via a UV momentum cutoff Λ. Thus we have introduced a new free parameter into the calculation. This was bound to happen in one form or another, since even in the renormalized perturbation theory one must introduce a new dimensional quantity (the "renormalization scale/point") at the one loop level. We treat this model as an effective theory and thus keep the cutoff without renormalization.*)

3.2. *The gap equations*

We vary the energy density with respect to the field vacuum expectation values $\langle\phi_i\rangle$ and the "dressed" masses m_i. The extremization condition with respect to the field vacuum expectation values reads

$$\left(\frac{\partial\mathcal{E}(m_i,\langle\phi_i\rangle)}{\partial\langle\phi_i\rangle}\right)_{\min}=0;\quad i=0,\cdots3$$

or

$$\begin{aligned}\left(\frac{\partial\mathcal{E}(m_i,\langle\phi_i\rangle)}{\partial\langle\phi_0\rangle}\right)_{\min}&=-\varepsilon+\langle\phi_0\rangle\left[-\mu_0^2+\lambda_0\left(\langle\boldsymbol{\phi}\rangle^2+3\hbar I_0(m_0)+\hbar\sum_{i=1}^{3}I_0(m_i)\right)\right]_{\min}\\&=0\ ,\\\left(\frac{\partial\mathcal{E}(m_i,\langle\phi_i\rangle)}{\partial\langle\phi_{j=1,2,3}\rangle}\right)_{\min}&=\langle\phi_j\rangle\left[-\mu_0^2+\lambda_0\left(\langle\boldsymbol{\phi}\rangle^2+\hbar\sum_{j\neq k=0}^{3}I_0(m_k)+3\hbar I_0(m_j)\right)\right]_{\min}\\&=0\ .\end{aligned} \qquad (3\cdot5)$$

Note that if we assume that $\langle\phi_0\rangle$ and $\langle\phi_{1,2,3}\rangle$ are simultaneously nonzero in the chiral limit $\varepsilon\to0$, then after subtracting one of the equations (3·5) from the other, we

*) There are several renormalization schemes for the Gaussian approximation, but as their names ("precarious" and "autonomous") suggest, they are unstable. [8)]

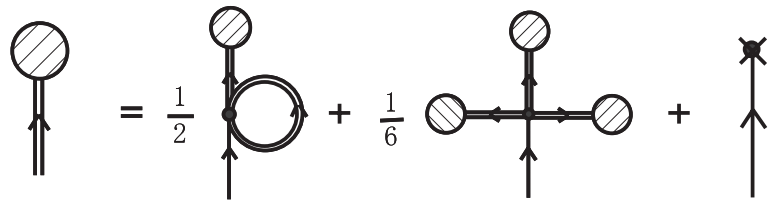

Fig. 1. The one-point Green function Schwinger-Dyson equation determining the dynamics of the σ model in the Hartree approximation: the one-loop graph (a), and the tree tadpole diagram (b). The solid line denotes the bare meson multiplet, and the double solid line is the dressed meson multiplet. The shaded blob together with the double line leading to it (the "tadpole") denotes the vacuum expectation value of the field (i.e. the one-point Green function), and the solid dot in the intersection of the four lines denotes the bare four-point coupling. The diagrams are explicitly multiplied by their symmetry numbers.

are forced to conclude that $I_0(M = m_0) = I_0(\mu = m_{1,2,3})$, or that these two masses are identical. This, however, leads one to the symmetric phase of the theory, so we must ignore this possibility. Instead, we assume only one $\langle\phi_i\rangle$ to be nonzero, e.g. $\langle\phi_0\rangle = v \neq 0$, while $\langle\phi_{1,2,3}\rangle = 0$. Thus the first set of energy minimization equations in the Gaussian variational approximation [7] reads

$$\mu_0^2 = -\frac{\varepsilon}{v} + \lambda_0 \left[v^2 + 3\hbar I_0(M) + 3\hbar I_0(\mu)\right] \ , \tag{3·6a}$$

$$\langle\phi_i\rangle = 0 \ , \quad i = 1, 2, 3 \ , \tag{3·6b}$$

where the divergent integral $I_0(m_i)$ is understood to be regularized via a UV momentum cutoff Λ, either three dimensional or four dimensional.

Equations (3·6a) and (3·6b) can be identified with the truncated Schwinger-Dyson (SD) equations [4] for the one-point Green function (see Fig. 1). We associate the nonvanishing vacuum expectation value (v.e.v.) with the "sigma meson" field ϕ_0, whose apparent mass is given by $m_0 = M$, and the remaining three fields $\phi_i (i = 1, 2, 3)$, of mass $m_i = \mu$, form the pion triplet. The second set of energy minimization equations reads

$$\begin{aligned} M^2 &= -\mu_0^2 + \lambda_0 \left[2\langle\phi_0\rangle^2 + \langle\boldsymbol{\phi}\rangle^2 + 3\hbar I_0(M) + 3\hbar I_0(\mu)\right] \\ &= -\mu_0^2 + \lambda_0 \left[3v^2 + 3\hbar I_0(M) + 3\hbar I_0(\mu)\right] \ , \end{aligned} \tag{3·7a}$$

$$\begin{aligned} \mu^2 &= -\mu_0^2 + \lambda_0 \left[\langle\boldsymbol{\phi}\rangle^2 + \hbar I_0(M) + 5\hbar I_0(\mu)\right] \\ &= -\mu_0^2 + \lambda_0 \left[v^2 + \hbar I_0(M) + 5\hbar I_0(\mu)\right] \ . \end{aligned} \tag{3·7b}$$

Equations (3·7a) and (3·7b) also have the Feynman-diagrammatic interpretation shown in Fig. 2. Upon inserting Eqs. (3·6a) and (3·6b) into Eqs. (3·7a) and (3·7b), the following two coupled "gap" equations emerge:

$$M^2 = \frac{\varepsilon}{v} + 2\lambda_0 v^2 \ , \tag{3·8a}$$

$$\mu^2 = \frac{\varepsilon}{v} + 2\lambda_0 \hbar \left[I_0(\mu) - I_0(M)\right] \ . \tag{3·8b}$$

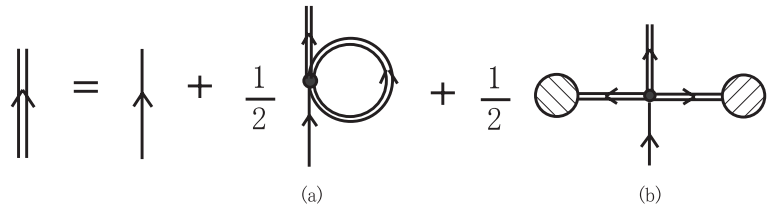

Fig. 2. Two-point Green function Schwinger-Dyson equation: the one-loop graph (a), and the tree tadpole diagram (b). The symbols have the same meaning as in Fig. 1.

One might be tempted to identify μ with the pion mass and M with the σ mass, then solve these equations and stop there. However, with $\varepsilon = 0$ these equations admit only massive solutions $M > \mu > 0$ for real, positive values of λ_0 and μ_0^2 and any real ultraviolet cutoff Λ in the momentum integrals $I_0(m_i)$ and $I_1(m_i)$ as these are positive definite (for any real mass). In other words, the "pion" (ϕ_1, ϕ_2 and ϕ_3) excitations are massive, with mass $\mu \neq 0$, in MFA, even in the chiral limit. This looks like a breakdown of the $O(4)$ invariance of this method, but, as discussed at length in Ref. 7), there is a simple solution obtained using the Bethe-Salpeter equation.*) Before proceeding to solve the gap equations (3·8a) and (3·8b), we will have to determine the value of the ε parameter in terms of observables calculated in the Gaussian approximation. For this purpose we also have to use the Bethe-Salpeter equation.

3.3. *The Bethe-Salpeter equation ("RPA"): $\sigma\pi$ scattering*

In Ref. 7) we showed that the Nambu-Goldstone particles appear as poles in the *two-particle propagator*; i.e., they are bound states of the two distinct massive elementary excitations in the theory. We specify the two-body dynamics in the theory in terms of the four-point SD equation or, equivalently, of the Bethe-Salpeter equation (see Figs. 3 and 4). We focus on the s-channel part $D_\pi(s)$ of the total four-point scattering amplitude $T(s,t,u)$. Its four-point SD equation reads

$$D_\pi(s) = V_\pi(s) + V_\pi(s) \Pi_\pi(s) D_\pi(s) \ , \tag{3·9}$$

$$\Pi_\pi(s) = I_{M\mu}(s) = i\hbar \int \frac{d^4k}{(2\pi)^4} \frac{1}{[k^2 - M^2 + i\epsilon]\,[(k-P)^2 - \mu^2 + i\epsilon]} \ , \tag{3·10}$$

$$V_\pi(s) = 2\lambda_0 \left[1 + \left(\frac{2\lambda_0 v^2}{s - \mu^2} \right) \right] = 2\lambda_0 \left[1 + \frac{M^2 - \frac{\varepsilon}{v}}{s - \mu^2} \right] \ , \tag{3·11}$$

with the solution

$$D_\pi(s) = \frac{V_\pi(s)}{1 - V_\pi(s)\Pi_\pi(s)} \ , \tag{3·12}$$

*) It is well known from the quantum many-body literature that the Hartree or mean-field approximation does not respect internal symmetries. The corrective measure goes by the name of random phase approximation (RPA).

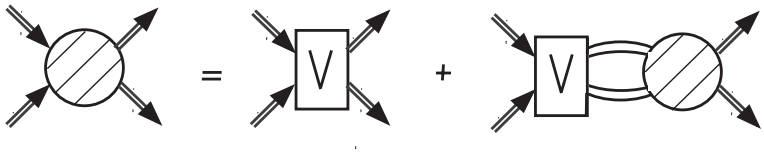

Fig. 3. Four-point Green function Schwinger-Dyson or Bethe-Salpeter equation. The square "box" represents the potential, and the round "blob" is the BS amplitude itself. All lines represent dressed fields like the double lines in Figs. 1 and 2.

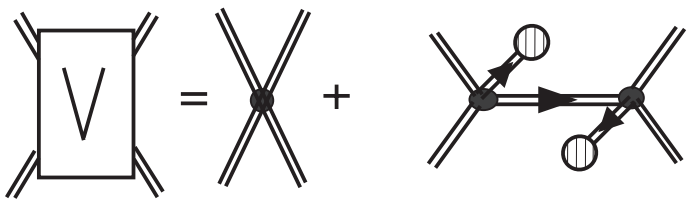

Fig. 4. The potential (square "box") entering the Bethe-Salpeter equation, as defined in the RPA.

where $s = (p_1 + p_2)^2 \equiv P^2$ is the center-of-mass (CM) energy. This propagator can also be written in the form (see Ref. 17))

$$D_\pi(s) \simeq \frac{g^2_{\pi\phi_i\phi_0}}{s - m^2_\pi}, \tag{3·13}$$

where

$$\begin{aligned} g^{-2}_{\pi\phi_i\phi_0} \equiv g^{-2}_{\rm eff} &= \left(\frac{1}{2\lambda_0(M^2-\mu^2)}\right)\left\{\left(\frac{M^2}{M^2-\mu^2}\right)\right. \\ &\left. + \frac{1}{(4\pi)^2}\left[\frac{1}{2} + \left(\frac{\mu^2}{M^2-\mu^2}\right)\left(1 - \left(\frac{M^2}{M^2-\mu^2}\right)\log\left(\frac{M^2}{\mu^2}\right)\right)\right]\right\} \\ &\simeq \left(\frac{M^2}{2\lambda_0(M^2-\mu^2)^2}\right) = \left(\frac{v}{M^2-\mu^2}\right)^2. \end{aligned} \tag{3·14}$$

We see that the second term in curly brackets is roughly 1% as large as the first one, and therefore we may neglect it in the first approximation.

Here we have simply presented the correct form of the four-point SD equation based on the truncation of the exact SD equation.[4)] The derivation from the Gaussian approximation in the symmetric phase of the theory can be found in Ref. 3). The corresponding derivation in the asymmetric (Nambu-Goldstone) phase can be found in Ref. 9). Furthermore, this BS equation is also the "random phase approximation" (RPA) equation of motion that describes "quasi-particles" in this theory (see Refs. 6), 9) and 10)).

3.4. *The Bethe-Salpeter equation: ππ scattering*

The dynamics are specified in terms of the SD, or equivalently, Bethe-Salpeter (BS) equation for the four-point Green functions $D_{ij}(s)$, where the indices i and j

denote the isospin of the pions in the initial and final states, respectively. We use the isospin invariance to split this 9×9 matrix equation into three invariant subspaces: (a) isoscalar, (b) isovector, and (c) isotensor. Because we consider S-wave scattering, the isovector amplitude vanishes identically, due to the Bose-Einstein statistics of the pions. The isotensor BS equation is linear and can be solved straightforwardly, but it is without distinguishing features. On the other hand, in the isoscalar channel we expect to see the σ meson. The corresponding BS equations consist of four coupled equations that can be put into 2×2 matrix form. [11)]

The main difference between the isoscalar channel and the pion channel, considered in §3.3, is that here we have two distinct intermediate states, one with two "elementary" sigma fields (ϕ_0) and the other with two "elementary" pion fields ($\phi_i, i = 1, 2, 3$). The isoscalar SD equations couple these two channels:

$$\begin{aligned}
D_{MM}(s) &= V_{MM}(s) + \frac{1}{2}V_{MM}(s)I_{MM}(s)D_{MM}(s) + \frac{3}{2}V_{M\mu}(s)I_{\mu\mu}(s)D_{\mu M}(s) \ , \\
D_{M\mu}(s) &= V_{M\mu}(s) + \frac{1}{2}V_{M\mu}(s)I_{\mu\mu}(s)D_{\mu\mu}(s) + \frac{1}{2}V_{MM}(s)I_{MM}(s)D_{M\mu}(s) \ , \\
D_{\mu M}(s) &= V_{\mu M}(s) + \frac{1}{2}V_{\mu M}(s)I_{MM}(s)D_{MM}(s) + \frac{1}{2}V_{\mu\mu}(s)I_{\mu\mu}(s)D_{\mu M}(s) \ , \\
D_{\mu\mu}(s) &= V_{\mu\mu}(s) + \frac{1}{2}V_{\mu\mu}(s)I_{\mu\mu}(s)D_{\mu\mu}(s) + \frac{3}{2}V_{\mu M}(s)I_{MM}(s)D_{M\mu}(s) \ . \qquad (3\cdot15)
\end{aligned}$$

The equations in (3·15) can be cast into matrix form as

$$\boldsymbol{D}_\sigma = \boldsymbol{V} + \frac{1}{2}\boldsymbol{V}\ \boldsymbol{\Pi}\ \boldsymbol{D}_\sigma \ , \qquad (3\cdot16)$$

$$\boldsymbol{D}_\sigma \equiv \begin{pmatrix} D_{MM} & D_{M\mu} \\ D_{\mu M} & \frac{1}{3}D_{\mu\mu} \end{pmatrix} \ , \qquad (3\cdot17)$$

where the boldfaced symbols are matrices. The solution to the matrix equation (3·16) is

$$\boldsymbol{D}_\sigma = (1 - \frac{1}{2}\boldsymbol{V}\ \boldsymbol{\Pi})^{-1}\ \boldsymbol{V} \ , \qquad (3\cdot18)$$

where

$$\begin{aligned}
\boldsymbol{V} &= \begin{pmatrix} V_{MM} & V_{M\mu} \\ V_{\mu M} & \frac{1}{3}V_{\mu\mu} \end{pmatrix} \\
&= 2\lambda_0 \begin{pmatrix} 3\left[1 + 3\frac{M^2 - \frac{\varepsilon}{v}}{s - M^2}\right] & \left[1 + 3\frac{M^2 - \frac{\varepsilon}{v}}{s - M^2}\right] \\ \left[1 + 3\frac{M^2 - \frac{\varepsilon}{v}}{s - M^2}\right] & \left[5 + 3\frac{M^2 - \frac{\varepsilon}{v}}{s - M^2}\right] \end{pmatrix} \ , \qquad (3\cdot19)
\end{aligned}$$

and

$$\boldsymbol{\Pi} = \begin{pmatrix} I_{MM} & 0 \\ 0 & 3\,I_{\mu\mu} \end{pmatrix} \ . \qquad (3\cdot20)$$

The invariant functions $I_{ii}(s)$ and $J_{ii}(s)$ are given by

$$\begin{aligned} I_{ii} &= i \int \frac{d^4k}{(2\pi)^4} \frac{1}{\left[k^2 - m_i^2 + i\varepsilon\right]\left[(k-P)^2 - m_i^2 + i\varepsilon\right]} \\ &= I_{ii}(0) + \frac{s}{(4\pi)^2}\left(-1 + J_{ii}(s)\right) \ , \end{aligned} \tag{3·21}$$

where $s = P^2$, and the real and imaginary parts of $J_{ii}(s)$ are

$$J_{ii}(s) = \begin{cases} \sqrt{\dfrac{4m_i^2}{s} - 1}\ \arcsin\left(\sqrt{\dfrac{s}{4m_i^2}}\right) \ , & \left(0 < \dfrac{s}{4m_i^2} < 1\right) \\ \sqrt{1 - \dfrac{4m_i^2}{s}}\ \left[\log\left(\sqrt{\dfrac{s}{4m_i^2}} + \sqrt{\dfrac{s}{4m_i^2} - 1}\right) - i\,\dfrac{\pi}{2}\right] \ . & \left(1 \le \dfrac{s}{4m_i^2} < \infty\right) \end{cases} \tag{3·22}$$

The equal mass integrals at zero momentum $I_{ii}(0)$ are cutoff-dependent constants ("subtraction constants" in the dispersion relations language) whose values are determined by the solutions M, μ and Λ to the gap equation (5·1). Thus, fixing of the subtraction constants is one of the primary consequences of the self-consistent gap equations. We use

$$I_{ii}^{(4)}(0) = (4\pi)^{-2}\left[\frac{x_4}{x_4+1} - \log(x_4+1)\right] \ ; \quad x_4 = \left(\frac{\Lambda_4}{m}\right)^2 \ , \tag{3·23a}$$

$$I_{ii}^{(3)}(0) = 2(4\pi)^{-2}\left[\frac{x_3}{\sqrt{x_3(1+x_3)}} - \ln(\sqrt{x_3} + \sqrt{1+x_3})\right]; \ x_3 = \left(\frac{\Lambda_3}{m}\right)^2 \ . \tag{3·23b}$$

Thus self-consistency of the gap equations enters into the scattering problem and constrains the remaining free parameters.

We see from Eq. (3·15) that in order to calculate the D_{MM} amplitude, we need to know the $D_{\mu M}(s)$ amplitude, and *vice versa*. In other words, we must solve the system of four coupled equations (3·15). It turns out that this system splits into two systems with two unknowns, with the same discriminant $\mathcal{D}$. This fact, (a) ensures that there are at most two poles in the solutions, and (b) greatly simplifies the algebra. The solutions to the equations (3·15) are

$$\begin{aligned} D_{MM}(s) &= \frac{1}{\mathcal{D}(s)}\left(V_{MM}(s) - 12\lambda_0 I_{\mu\mu}(s) V_{M\mu}(s)\right) \ , \\ D_{\mu\mu}(s) &= \frac{1}{\mathcal{D}(s)}\left(V_{\mu\mu}(s) - 12\lambda_0 I_{MM}(s) V_{M\mu}(s)\right) \ , \\ D_{\mu M}(s) &= D_{M\mu}(s) = \frac{1}{\mathcal{D}(s)} V_{M\mu}(s) = \frac{1}{\mathcal{D}(s)} V_{\mu M}(s) \ , \end{aligned} \tag{3·24}$$

where

$$\mathcal{D}(s) = 1 - \frac{1}{2}\left[V_{MM}(s) I_{MM}(s) + V_{\mu\mu}(s) I_{\mu\mu}(s)\right] + 6\lambda_0 I_{MM}(s) I_{\mu\mu}(s) V_{\mu M}(s) \tag{3·25}$$

is the discriminant of "one half" of the system of Eq. (3·15). Elementary and composite states in the s-channel manifest themselves as poles in the $\boldsymbol{D}_\sigma(s)$ matrix, or equivalently as roots of

$$(s - M^2)\mathcal{D}(s) = 0. \tag{3·26}$$

This equation is identical to the formula for the σ mass in the optimized perturbation theory (OPT).[12)]

An inspection of Eq. (3·25) leads one to think that $(s - M^2)\mathcal{D}(s)$ should be a quadratic polynomial (function) of s and therefore have two roots, since each $(s-M^2)V_{ij}(s)$ is a linear function of s. However, as a consequence of chiral symmetry, one finds that the function $(s - M^2)\mathcal{D}(s)$ is (only) linear in s. This, in turn, ensures that there is only one root of the "eigenvalue" equation (3·26), and hence only one pole in the σ propagator at least for small values of s, where the I_{ii} functions' logarithmic s dependence may be neglected. For large values of s, this is no longer the case, as we show in §5.

§4. Chiral symmetry Ward identities in the Gaussian approximation

Chiral Ward-Takahashi identities follow from the underlying chiral symmetry of the linear sigma model and typically relate (n-1)-point Green functions to other n-point functions and/or currents. These identities were developed by Lee at the perturbative one loop level,[13)] and by Symanzik at arbitrary orders of perturbation theory.[14)] We call them the Lee-Symanzik [LS] identities. To our knowledge, for selected infinite classes of diagrams in the linear sigma model no proofs of LS identities were given prior to Ref. 7). The NG theorem is the simplest LS identity. When the chiral symmetry is explicitly broken, NG theorem turns into a relation between the chiral symmetry-breaking parameter and the NG boson mass, as first discussed by Dashen.[15)] The NG theorem in the chiral limit has already been addressed in the Gaussian approximation and related formalisms in Refs. 7), 6) and 16). For this reason, we consider the nonchiral case.

4.1. *Dashen's formula and the Nambu-Goldstone theorem*

As shown in Ref. 7), in the chiral limit the Nambu-Goldstone particle appears as a zero-mass pole in the pion channel *two-particle propagator* Eq. (3·12). Next, we consider the zero CM energy $P = 0$ polarization function $V_\pi(0)\Pi_\pi(0)$ in the nonchiral case. We use Eq. (3·7b) to write

$$\begin{aligned} V_\pi(0)\Pi_\pi(0) &= \frac{2\lambda_0\hbar}{(M^2-\mu^2)}\left[I_0(M) - I_0(\mu)\right]\left[1 - \frac{M^2 - \frac{\varepsilon}{v}}{\mu^2}\right] \\ &= \left(\frac{\frac{\varepsilon}{v} - \mu^2}{M^2-\mu^2}\right)\left[1 - \frac{M^2 - \frac{\varepsilon}{v}}{\mu^2}\right] \end{aligned} \tag{4·1}$$

and then use Eq. (3·7a) to obtain the final result,

$$V_\pi(0)\Pi_\pi(0) = 1 - \frac{\varepsilon}{v}\left(\frac{M^2}{\mu^2(M^2-\mu^2)}\right) + \mathcal{O}(\varepsilon^2) \quad . \tag{4·2}$$

The propagator Eq. (3·12) evaluated at zero momentum can be written as

$$D_\pi(0) \simeq \frac{g^2_{\pi\phi_i\phi_0}}{-m^2_\pi} = -\left(\frac{2\lambda_0}{m^2_\pi}\right)\left(\frac{M^2-\mu^2}{M^2}\right)^2$$
$$= \frac{V_\pi(0)}{1-V_\pi(0)\Pi_\pi(0)} = -2\lambda_0\left(\frac{v}{\varepsilon}\right)\left(\frac{M^2-\mu^2}{M^2}\right)^2 , \qquad (4\cdot3)$$

which leads to the result $\varepsilon = m^2_\pi v + \mathcal{O}(\varepsilon^2)$. This is also in agreement with a general result due to Dashen.[15] The vacuum expectation value of the Σ operator, when sandwiched between two vacuum states, yields Dashen's formula,

$$\Big(fm^2f\Big)^{ab} = f_a m^2_{ab} f_b = -\langle 0\,\Big|\Big[Q^a_5,[Q^b_5,\mathcal{H}_{\chi\mathrm{SB}}]\Big]\Big|\,0\rangle + \mathcal{O}(m^4_\pi) , \qquad (4\cdot4)$$

for the pseudoscalar meson mass squared (m^2_{ps}) and decay constant f_a for an arbitrary chiral symmetry-breaking term in the Hamiltonian density $\mathcal{H}_{\chi\mathrm{SB}}$. This is a model-independent result based on the equations of motion in the Heisenberg representation and on the LSZ reduction formulas. We use the canonical commutation relations and the axial charge to evaluate the Σ operator in the linear Σ model,

$$\Sigma\delta^{ab} = \Big[Q^a_5,[Q^b_5,\mathcal{H}_{\chi\mathrm{SB}}(0)]\Big] = -\varepsilon\sigma\delta^{ab} , \qquad (4\cdot5)$$

which vanishes when the chiral symmetry is not explicitly broken. Taking the vacuum expectation value of this expression, we find

$$(m_\pi f_\pi)^2 = \varepsilon\langle 0\,|\sigma|\,0\rangle + \mathcal{O}(\varepsilon^2) , \qquad (4\cdot6)$$

which leads to

$$\varepsilon = m^2_\pi f_\pi \quad . \qquad (4\cdot7)$$

This relation is satisfied both in the Born and Gaussian approximations, which indicates that both are chirally symmetric. Now that ε has been fixed, note that the gap equation (3·8b) implies $m^2_\pi \le \mu^2$, in agreement with the variational nature of the Gaussian approximation. This is important in the numerical calculations discussed below and for the physical interpretation.

4.2. *Axial current Ward identity*

The axial current matrix element corresponding to the Feynman diagrams displayed in Fig. 5 reads

$$J^a_{\mu5}(p',p) = \langle\phi^a(p')|J_\mu(0)|\phi_0(p)\rangle$$
$$= (p'+p)_\mu + q_\mu\left(\frac{M^2-\frac{\varepsilon}{v}}{q^2-\mu^2}\right)$$
$$-\Gamma_{\mu5}(q)D_\pi(q) , \qquad (4\cdot8)$$

where $\Gamma_{\mu5}(q)$ is defined by

$$\Gamma_{\mu5}(q) = i\int\frac{d^4k}{(2\pi)^4}\left[(2k+q)_\mu + q_\mu\left(\frac{M^2-\frac{\varepsilon}{v}}{q^2-\mu^2}\right)\right]\frac{1}{[k^2-M^2]\,[(k+q)^2-\mu^2]} \qquad (4\cdot9)$$

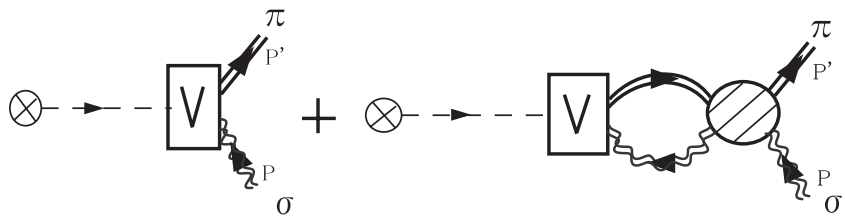

Fig. 5. Axial current matrix element.

and satisfies the chiral Ward identity, [18]

$$q^\mu \Gamma_{\mu 5}(q) = \left[\frac{\mu^2}{2\lambda_0} \left(V_\pi(0) \Pi_\pi(0) - V_\pi(q^2) \Pi_\pi(q^2) \right) - \frac{\varepsilon}{v} \left(\Pi_\pi(0) - \Pi_\pi(q^2) \right) \right] \ . \tag{4·10}$$

We insert the vertex $\Gamma_{\mu 5}(q)$ in Eq. (4·9) together with the two-body propagator $D_\pi(q^2)$ in Eq. (3·12) into Eq. (4·8) to find

$$\begin{aligned} J_{\mu 5}(p^{'}, p) &= (p^{'} + p)_\mu + q_\mu \left(\frac{M^2 - \frac{\varepsilon}{v}}{q^2 - \mu^2} \right) \\ &\quad - \frac{q_\mu}{q^2} \left[\frac{\mu^2}{2\lambda_0} \left(V_\pi(0) \Pi_\pi(0) - V_\pi(q^2) \Pi_\pi(q^2) \right) - \frac{\varepsilon}{v} \left(\Pi_\pi(0) - \Pi_\pi(q^2) \right) \right] \\ &\quad \times \left(\frac{V_\pi(q^2)}{1 - V_\pi(q^2) \Pi_\pi(q^2)} \right) \\ &\simeq (p^{'} + p)_\mu + q_\mu \left(\frac{M^2 - \mu^2 - m_\pi^2}{q^2 - m_\pi^2} \right) \ . \end{aligned} \tag{4·11}$$

Here we have $q^\nu = (p^{'} - p)^\nu$. This result manifestly lacks a pole at $q^2 = \mu^2$. The composite state plays precisely the role of the Nambu-Goldstone boson in the conservation of the (axial) Noether current, i.e., in the basic axial Ward-Takahashi identity

$$q^\nu J_{\nu 5}(p^{'}, p) = \left(p^{'2} - \mu^2 \right) - \left(p^2 - M^2 \right) + m_\pi^2 \left(\frac{M^2 - \mu^2 - m_\pi^2}{q^2 - m_\pi^2} - 1 \right) \ , \tag{4·12}$$

which follows directly from Eq. (4·11). Furthermore, f_π is defined by

$$\langle 0 | J_{\mu 5} | \Pi(\boldsymbol{q}) \rangle = f_\pi(q) q_\mu = g^{\text{eff}} \Gamma_{\mu 5}(q), \tag{4·13}$$

from which (in the chiral limit) it follows that

$$f_\pi(0) g^{\text{eff}} = M^2 - \mu^2, \tag{4·14}$$

by way of the axial Ward identity Eq. (4·10). This result, together with Eq. (3·14) for g^{eff} forms the basic result for the composite pion decay constant,

$$f_\pi = f_\pi(0) = g_{\text{eff}}^{-1} \left(M^2 - \mu^2 \right) = v \left[1 + \mathcal{O}\left((4\pi)^{-2} \right) \right] \simeq v. \tag{4·15}$$

§5. Numerical solutions

5.1. *The self-consistency or gap equation*

Having determined the value of the parameter $\varepsilon = vm_\pi^2$ in terms of observables, we can solve the gap equations. We fix the v.e.v. v at a value of 93 MeV for the pion decay constant f_π and a value of 140 MeV for the physical pion mass m_π. As a result, the system of gap equations (3·8a) and (3·8b) turns into a single equation:

$$\begin{aligned} v^2 = f_\pi^2 &= \left(\frac{M^2 - \frac{\varepsilon}{v}}{\mu^2 - \frac{\varepsilon}{v}}\right) \hbar \left[I_0(\mu) - I_0(M)\right] \\ &= \left(\frac{M^2 - m_\pi^2}{\mu^2 - m_\pi^2}\right) \hbar \left[I_0(\mu) - I_0(M)\right] \ . \end{aligned} \tag{5·1}$$

Here, we have used Eq. (3·3) as the integral to be regulated. We give here the results for (covariant) four-dimensional Euclidean cutoff regularization the three-dimensional regularization of this quadratically divergent integral:

$$I_0^{(4)}(m^2) = (4\pi)^{-2} m^2 \left[x_4 - \ln(1 + x_4)\right] \ ; \quad x_4 = \left(\frac{\Lambda_4}{m}\right)^2 \ , \tag{5·2a}$$

$$I_0^{(3)}(m^2) = 2(4\pi)^{-2} m^2 \left[\sqrt{x_3(1 + x_3)} - \ln(\sqrt{x_3} + \sqrt{1 + x_3})\right] ; \ x_3 = \left(\frac{\Lambda_3}{m}\right)^2 \ . \tag{5·2b}$$

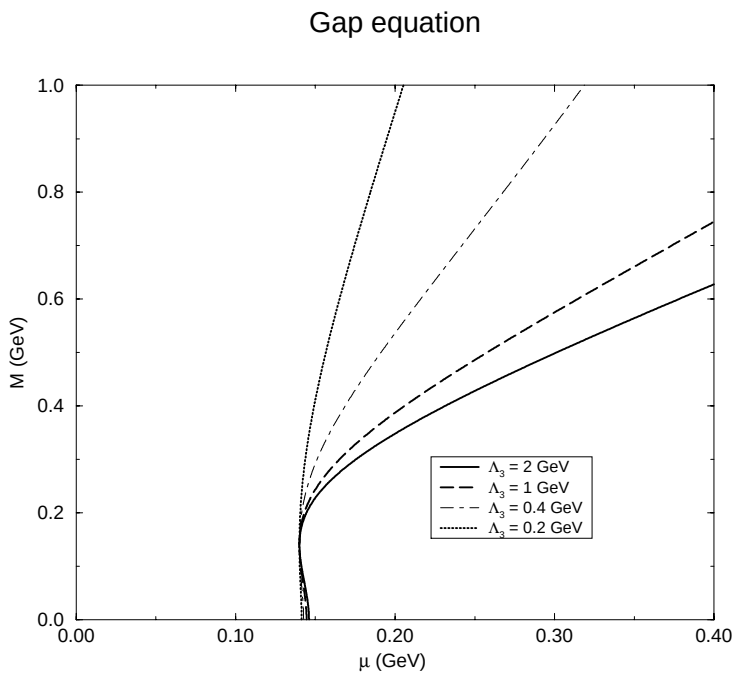

Fig. 6. Solutions to the nonchiral gap equation in the Gaussian approximation to the $O(4)$ linear sigma model with different values of the (three-dimensional) cutoff Λ_3.

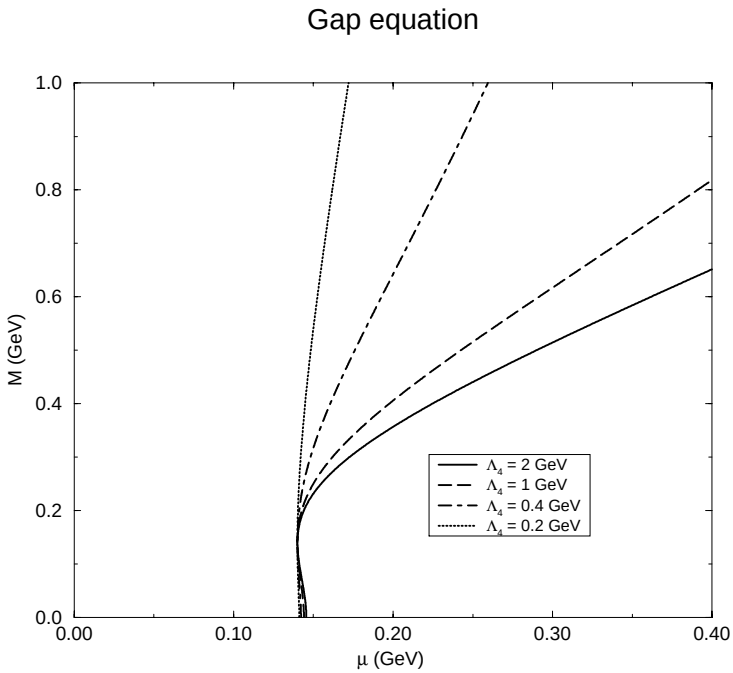

Fig. 7. Solutions to the nonchiral gap equation in the Gaussian approximation to the $O(4)$ linear sigma model with different values of the (four-dimensional) cutoff Λ_4.

Note that the $\hbar \to 0$ limit of Eq. (5·1) is non-trivial: on the right-hand side, both the numerator and the denominator vanish. Further, note that one parameter, in this case the cutoff Λ, remains free.

Numerical solutions to the equation (5·1) are plotted in Figs. 6 and 7 for various values of the cutoff Λ. Every point on the (μ, M) curve represents a solution to the gap equation, thus signalling the existence of freedom of choice in the form of one continuous free parameter. This free parameter can be related to the bare coupling constant λ_0 by Eq. (3·8a) for every (μ, M) pair.

In Figs. 6 and 7 we see that as the cutoff Λ increases, all solutions to the gap equation approach the symmetry restoration limit $M \to \mu$ for large values of M, or equivalently large values of λ_0. This implies that the large boson loop effects lead to symmetry restoration, in contrast to the fermion loops, which lead to symmetry breaking. Solutions that lie above the 2μ threshold require rather small values of (either kind of) cutoff Λ. However, this is in agreement with the small (second) meson-loop cutoff found in $1/N_c$ studies of the NJL chiral quark model.[19] This does not mean that the loop effects are necessarily small, however.

5.2. *The Bethe-Salpeter or scattering equation*

We reduced the BS equation (3·15) in the isoscalar channel to solving a single algebraic equation (3·26) involving the transcendental analytic functions $I_{MM}(s)$ and

$I_{\mu\mu}(s)$ with branch cuts at imaginary parts above the corresponding thresholds.*) This equation has, in general, real and imaginary parts: For σ mass values lying below the two-body threshold, only the real part is relevant, while for heavier σ masses the imaginary part must be taken into account as well. The latter determines the natural decay width of the σ meson.

From numerical solutions to the real part of Eq. (3·26) shown in Fig. 8, it can be seen that the σ mass is always shifted *downward* from the "elementary" sigma field (ϕ_0) mass M, in agreement with the variational property of the mean-field approximation. For small values of M ($\leq 2\mu$) (i.e., when the coupling constant λ_0 lies below some critical value λ_c, which is a function of the masses μ, M and the cutoff Λ), the σ meson mass (i.e., the real part of the pole position) drops below the 2μ threshold, and the σ meson comes to consist predominantly of the bare ϕ_0 state with some 2π and 2σ "cloud" components admixed to its wave function.**) With increasing coupling constant λ_0, the physical σ's mass increases above the 2μ threshold, and the "bare" and "dressed" components of the wave function can no longer be separated. Then, the state itself must be considered as predominantly a meson-meson composite. For weak couplings, only one state has been found to exist in the σ channel of the MFA. In Fig. 8 it can be seen that the σ mass changes continuously with decreasing coupling λ_0 and connects smoothly to the perturbative σ mass in the weak coupling limit.

Note, further, that for many values of the cutoff Λ and above some critical value of M, far into the 2μ continuum, there is a second root of the real part of Eq. (3·26). As increases $M \sim \sqrt{\lambda_0}$, the two roots sometimes merge into one and then immediately disappear (see Fig. 9). For other values of the parameters, the two roots diverge, the smaller one moving down to zero, while the heavier one moves back up in mass again. In either case, the smaller zero, which is connected to the perturbative solution, has an upper limit generally below 1 GeV. This is perhaps the most interesting result of this paper. We remind the reader that these results are not artifacts of the Gaussian approximation viewpoint, as exactly the same equations govern the OPT meson masses.

The question of the physical meaning of the two zeros arises; i.e., if actual poles exist on the second unphysical Riemann sheet of the S-matrix that can be associated with these zeros in the real part of the inverse propagator? The larger zero is almost certainly not a conventional pole, because the derivative of Eq. (3·26) evaluated at the root has sign opposite to that at the smaller root. Because this derivative is related to the effective coupling constant squared, this implies that the upper state has a non-Hermitian coupling to the bare states. This question is more difficult to address, as it demands analytic continuation onto the second Riemann sheet. It will be left to a future investigation.

*) $I_{MM}(s)$ and $I_{\mu\mu}(s)$ have logarithmic branch points and therefore infinitely many sheets, in contrast with the nonrelativistic case, in which the branch points are of the square root type, with only two sheets.

**) Another interpretation of these results (that might be only semantically different from that one) has been given in the language of operator many-body ("quasi-particle RPA") methods.[6),10)]

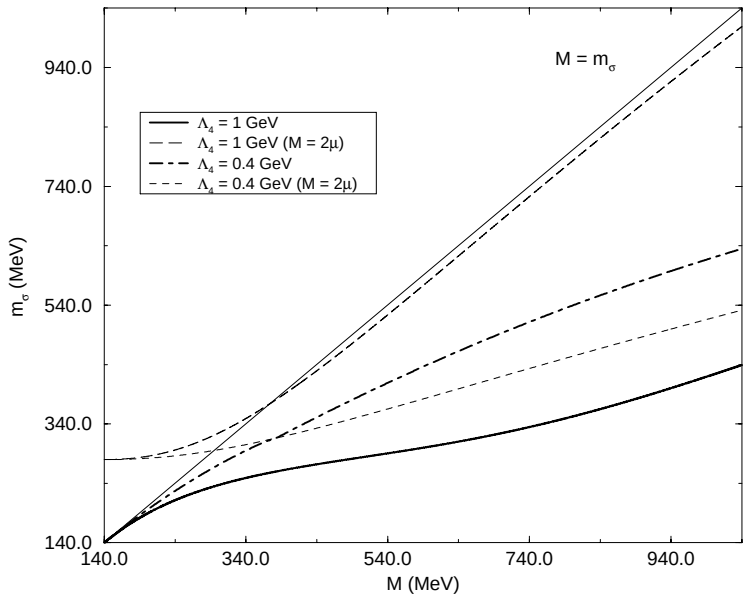

Fig. 8. The solution m_σ to the Bethe-Salpeter equation in the isoscalar channel as a function of the variational parameter M for various values of the cutoff, Λ. The curves denoted 2μ show the movement of the 2μ threshold for corresponding values of the parameters M and Λ.

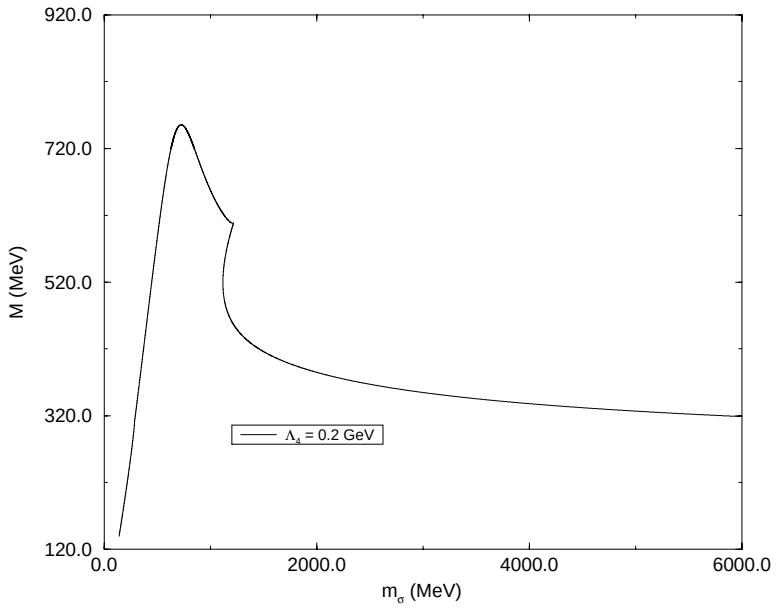

Fig. 9. The solution m_σ to the Bethe-Salpeter equation in the isoscalar channel as a function of the variational parameter M for a small cutoff, $\Lambda = 0.2$ GeV. Note the double-valued nature of these functions, as well as the absence of solutions above certain values of M.

§6. Summary and conclusions

In summary, we have: 1) constructed a unitary, Lorentz and chirally invariant, self-consistent variational approximation to the linear σ model; 2) solved the coupled self-consistent equations of motion in this, the mean-field plus random-phase approximation (MFA + RPA). The solutions to these equations also determine the minimum of the "optimized perturbation theory" effective potential.; 3) shown that the particle content of the mean-field plus random-phase approximation to the $O(4)$ linear sigma model is the same as in the Born approximation, at least for weak coupling, i.e., there are three Goldstone bosons π and one σ state. 4) found that the pions' mass is unchanged, as a consequence of the validity of Dashen's relation in the MFA + RPA, whereas the σ mass and width can differ substantially from the Born values, depending on the free parameters. 5) calculated the σ meson mass by solving the nonperturbative Bethe-Salpeter equation. We found a second solution for large values of mass and coupling, whose physical interpretation is yet unclear.

The mean-field or Gaussian method was initially fraught with problems when applied to the linear σ model with spontaneously broken internal symmetry — the Goldstone theorem did not seem to "work". This problem was solved in Ref. 7): The Goldstone boson found in the Gaussian approximation [7)] turns out to be a composite massless state, just as in the NJL model. Yet, there seemed to exist another massive state with the quantum numbers of the pion. In fact, however, this is true only in appearance: There is no pole in the propagator corresponding to this "particle". The MFA to the bosonic linear σ model is significantly different from the NJL one in one regard: Whereas in the NJL model, the gap equation describes "dressing" of the fermions and the BS equation describes mesons as bound states of dressed fermions, in the linear σ model both the gap and the BS equations describe (two different) "dressings" (first and second renormalizations) of mesons. Therefore, the results of the intermediate (first) renormalization remain in the theory even after the second renormalization and confuse the issues of the physical content. A more complicated situation exists in the scalar sector. We have not yet written the last word on this subject.

We hope to extend these calculations to physical applications for more realistic Lagrangians in the future.

Acknowledgements

One of the authors [V. D.] would like to acknowledge a Center-of-Excellence (COE) Professorship for the year 2000/1 and the hospitality of RCNP. We wish to acknowledge the kind help in all matters concerning computers and software that we received from Ms. Miho Takayama-Koma, as well as help with Canvas software from Dr. F. Araki. The authors wish to thank Professor H. Toki for introducing them.

References

1) B. W. Lee, *Chiral Dynamics* (Gordon and Breach, New York, 1972).
2) J. L. Basdevant and B. W. Lee, Phys. Rev. D **2** (1970), 1680.

K. S. Jhung and R. S. Willey, Phys. Rev. D **9** (1974), 3132.
W. Lin and B. Serot, Nucl. Phys. A **512** (1990), 650.
3) T. Barnes and G. I. Ghandour, Phys. Rev. D **22** (1980), 924; see also
Variational Calculations in Quantum Field Theory, ed. L. Polley and D. E. L. Pottinger (World Scientific, Singapore, 1987).
4) R. J. Rivers, *Path Integral Methods in Quantum Field Theory* (Cambridge University Press, Cambridge, 1987).
B. Hatfield, *Quantum Field Theory of Point Particles and Strings* (Addison-Wesley, Reading, 1992).
5) S. Chiku and T. Hatsuda, Phys. Rev. D **57** (1998), R 6; D **58** (1998), 076001.
H.-S. Roh and T. Matsui, Eur. Phys. J. A **1** (1998), 205.
J. T. Lenaghan, D. H. Rischke and J. Schaffner-Bielich, Phys. Rev. D **62** (2000), 085008.
Y. Nemoto, K. Naito and M. Oka, Eur. Phys. J. A **9** (2000), 245.
6) H. W. L. Aouissat, O. Bohr and J. Wambach, Mod. Phys. Lett. A **13** (1998), 1827.
7) V. Dmitrašinović, J. A. McNeil and J. Shepard, Z. Phys. C **69** (1996), 359.
8) P. M. Stevenson, Phys. Rev. D **32** (1985), 1389; see also
P. M. Stevenson and R. Tarrach, Phys. Lett. B **176** (1986), 436.
P. M. Stevenson, Z. Phys. C **35** (1987), 467.
9) A. K. Kerman and Chi-Yong Lin, Ann. of Phys. **269** (1998), 55.
10) A. Fetter and J. D. Walecka, *Quantum Theory of Many-Body Systems* (McGraw-Hill, New York, 1971).
11) V. Dmitrašinović, Phys. Lett. B **433** (1998), 362.
12) A. Okopińska, Phys. Lett. B **375** (1996), 213.
13) B. W. Lee, Nucl. Phys. B **9** (1969), 649.
14) K. Symanzik, Comm. Math. Phys. **16** (1970), 48.
15) R. Dashen, Phys. Rev. **183** (1969), 1245.
R. Dashen and M. Weinstein, Phys. Rev. **183** (1969), 1261; **188** (1969), 2330.
16) Y. Tsue, D. Vautherin and T. Matsui, Phys. Rev. D **61** (2000), 076006.
17) F. Gross, *Relativistic Quantum Mechanics and Field Theory* (J. Wiley, N.Y., 1993).
18) V. Dmitrašinović, Nuovo. Cim. A **109** (1996), 1187.
19) V. Dmitrašinović, R. H. Lemmer, H. J. Schulze and R. Tegen, Ann. of Phys. **238** (1995), 332.
M. Oertel, M. Buballa and J. Wambach, Nucl. Phys. A **676** (2000), 247.